Supporting Material

Lateral dynamics of proteins with polybasic domain on anionic membranes: A dynamic Monte-Carlo study

Vladimir Yu. Kiselev, Davide Marenduzzo, and Andrew B. Goryachev

Supporting Methods

Testing and calibration of the automaton

The Monte-Carlo automaton defined above (see Model) has been extensively tested to ensure that it adequately represents the dynamics of the system at hand. Averaging results over several thousands of independent realizations, we computed $\langle x \rangle$, $\langle y \rangle$ and $\langle r^2 \rangle$ as a function of time (5000 time steps) for lipid trajectories initiated at the origin positioned in the center of the lattice. As expected, both $\langle x \rangle$ and $\langle y \rangle$ exhibited random fluctuations around 0 with time-independent amplitude that converged to zero with increasing statistics. The mean squared displacement (msd) of lipids scaled as $\langle r^2 \rangle \sim t^{\alpha}$ where $\alpha = 1$ with high precision over the entire simulation period. Thus, following microscopic moves defined above, lipids undergo isotropic Brownian diffusion without drift. For the physiologically relevant mole fractions of monovalent charged and neutral lipids (e.g., 25% PS and 75% PC) and in the absence of interacting peptides, the rejection rate of lipid dynamics was negligible suggesting that essentially all proposed lipid moves were accepted. We then repeated the same tests for Lys-5 peptide at various lipid concentrations to confirm that it also performed unbiased Brownian motion. Interestingly, the importance of rotational move became apparent with the addition of PIP_2. Already at the PIP_2 fraction exceeding 0.1%, the peptide sequesters appreciable negative charge that repels surrounding PS lipids. In the absence of rotation, the inherent geometric asymmetry of Lys-5 produced artificial net force that caused a systematic drift of the peptide in the direction defined by its orientation on the peptide lattice.

Diffusive dynamics of free lipids provides a natural method to calibrate our automaton. With chosen spatial period of the lattice, we typically considered square spatial domains with linear dimensions $80 - 240\,nm$ (100-300 nodes). From the dependence of the lipid msd on the number of time steps and the chosen target value for the free lipid diffusion coefficient (e.g., $D_L = 1\,\mu m^2/s$ for typical *in vivo* conditions) it is straightforward to estimate the "real world" Δt corresponding to one automaton time step. Thus, for the conservative estimate for the free lipid diffusion coefficient, $D_L = 1\,\mu m^2/s$, the corresponding $\Delta t = 0.22\,\mu s$ and is respectively smaller for the simulations aiming to reproduce dynamics in artificial lipid bilayers. Since within one automaton step the absolute majority of freely diffusing lipids succeed to move, no further rescaling of the automaton time, e.g., by the acceptance rate as suggested in (Sanz and Marenduzzo. 2010. J. Chem. Phys. 132:194102), is necessary.

To avoid non-local motion of the peptides that could result in potentially artificial non-physical consequences, we restricted maximal mobility of the peptide by the requirement that it can move at most one lattice period per time step. Thus, the lateral diffusion coefficient of the peptide is naturally capped by the maximal mobility when the rejection rate of the peptide motion is identically 0, which is achieved in the absence of any electrostatic interactions with lipids (100% neutral lipid). For simplicity, we denote this value in the following discussion as D_0 and utilize it as a scaling factor for the presentation of the results on the peptide lateral dynamics. Again, as in the lipid case, a suitable experimental value of D_0 can be used to convert all obtained results into the dimensional units. To achieve peptide lateral dynamics with diffusion coefficient smaller than the maximal, translational move was performed with the probability $\omega < 1$ resulting in the reduced diffusion coefficient ωD_0.

Simulation details

As a rule, periodic boundary conditions were imposed on the dynamics on both lipid and peptide lattices. However, to generate lipid gradients discussed below, charged lipids were inserted periodically on the left boundary and removed from the lattice once they approached the right boundary. Lateral dynamics of the peptide was followed once the steady state lipid gradient was achieved after cessation of transient lipid dynamics (at least 20000 automaton steps). To achieve constant concentration of monovalent lipid at the origin (lattice center) with varying values of the gradient, we introduced two lipid species with the same charge (-1) but distinct boundary conditions. The gradient was generated in the spatial distribution of one specie, whereas the other exhibited homogeneous distribution owing to the periodic boundary conditions.

All simulations were performed using custom written C code on a multiprocessor Dell Precision T7400 workstation.

Effective charge of a diffusing peptide

To derive the value of the effective charge (per peptide node) associated with the translocating peptide, we consider all possible elementary situations schematically represented in Fig. S1A. Here we assume that the peptide diffuses on the membrane consisting only of neutral and monovalent lipids (PS). As the molar fraction of PS, ρ, grows from 0 to 100%, the total charge of the peptide-lipid complex decreases from +1 to 0 as shown by the dashed line in Fig. S1B. If we denote the probability of a peptide node to be associated with PS as $p(\rho)$, then the total charge (per node) will be $0<1-p(\rho)<1$. Consider now one elementary move of the peptide node from the "old" position in the center of a hexagonal neighborhood shown in Fig. S1A to the "new" position in the left-upper corner of the neighborhood. Prior to the move, this lattice position was occupied with PS with the probability ρ, while the peptide node was bound to PS with the probability $p(\rho)$. We further assume that these two random events are independent of each other and thus mutual probabilities can be calculated as products of corresponding event probabilities. If a PS lipid was bound to the peptide node in the "old" position, it will be dragged by the node resulting in the Kawasaki swap with a lipid located in the "new" position prior to the move. All four potential elementary situations are depicted in Fig. S1A:

1. The peptide node is bound to PS and the "new" position is originally occupied by PS. The resulting move is equivalent to the translocation of a free peptide node (+1), thus effective charge associate with this move $Z_1 = +1$, and it occurs with probability $P_1 = p(\rho)\cdot\rho$.
2. The peptide node together with the associated PS translocate into the position that was occupied by a neutral lipid. Therefore, the effective translocating charge is $Z_2 = 0$ and the probability of this scenario is $P_2 = p(\rho)\cdot(1-\rho)$.
3. The peptide node is free in the "old" position and the new position is occupied by PS. Thus, $Z_3 = +1$ and $P_3 = (1-p(\rho))\cdot\rho$.
4. Neither the peptide node nor the "new" lattice position are associated with PS resulting in $Z_4 = +1$ and $P_4 = (1-p(\rho))\cdot(1-\rho)$.

As can be readily seen by enumeration, the four scenarios exhaust all the possibilities and the sum of all P_i is identical unity. Finally, the average density-dependent value of the translocating charge per one peptide node is given by:

$$Z(\rho) = \langle Z_i \rangle = \sum_{i=1}^{4} Z_i P_i = 1 - p(\rho)(1-\rho).$$

Supporting Discussion

Considering the hydrophobic core of the membrane has a minor influence on the predicted velocity of the peptide in a lipid gradient

While charged headgroups of lipids and amino acid residues of peptides interact well within the hydrated layer of the membrane, a more accurate description of the membrane would require considering the existence of the membrane core with a significantly smaller dielectric constant. To investigate how such a refinement might impact on our result for the drift velocity of the peptide in a lipid gradient (Eq. 9), we followed the approach developed by Tzlil *et al*. (Eq. 5 in Ref. 44, Biophys. J., 95:1745, 2008) on the basis of the original work by Netz (Phys. Rev. E., 60:3174, 1999). Within this framework, the interaction potential between two ionic charges in addition to the standard Debye-Hueckel type term of Eq. 1 has also an interface interaction term:

$$\frac{qq'}{4\pi\varepsilon\varepsilon_0}\frac{e^{-\frac{\sqrt{r^2+4zz'}}{\lambda}}}{\sqrt{r^2+4zz'}},$$

where q, q', λ, and r are as defined earlier in this work, while z and z' are the distances of the two charges from the interface between the hydrated and hydrophobic layers of the membrane.

To estimate the distances z and z', we resorted to a recent model of the lipid bilayer that calculates the profile of the membrane dielectric constant using explicit molecular dynamics simulation of the bilayer (Nymeyer & Zhou, Bioph. J., 94:1185, 2008). In agreement with the previously published data, this model demonstrates that the charged headgroups of phospholipids are located approximately 1 *nm* above the interface between the hydrated membrane layer with the dielectric properties of water and the hydrophobic core with much smaller dielectric constant. Given the geometry of our model and the assumption of the physiological ionic strength, z and z' are approximately equal and are both on the order of one Debye length ($\lambda \approx 1$ *nm*).

To assess the influence of this more detailed approximation on the peptide drift in a lipid gradient, the two-dimensional integral in Eqs. 4-6

$$\int_0^{2\pi} d\theta \int_0^{+\infty} drr\frac{e^{-\frac{r}{\lambda}}}{r}$$

should be replaced by

$$\int_0^{2\pi} d\theta \int_0^{+\infty} drr\left[\frac{e^{-\frac{r}{\lambda}}}{r}+\frac{e^{-\frac{\sqrt{r^2+4z^2}}{\lambda}}}{\sqrt{r^2+4z^2}}\right].$$

By noting that the primitive function of the second term is

$$-\lambda e^{-\frac{\sqrt{r^2+4z^2}}{\lambda}},$$

the integration can be still performed explicitly, and following the steps leading to Eq. 9 we find a new value for the drift velocity:

$$\vec{v} = -2\pi \frac{Zq}{e^2} l_B \lambda D_p \nabla \rho(\vec{r}^*)\left(1 + e^{-2z/\lambda}\right)$$

Comparing this expression with Eq. 9, we see an additional correction factor $\left(1+e^{-2z/\lambda}\right)$ which depends on the precise position of the charges relative to the dielectric interface. In agreement with observations of Ref. 44, this correction is maximal and equal to 2 when the charges are positioned exactly on the dielectric interface. Substituting $\lambda = z$, we find that, at least in our case, taking into the consideration the existence of the membrane dielectric core leads to a rather minor correction of approximately 14%.

Validation of the peptide drift in the lipid gradient

To further validate the effect of the peptide drift in the gradient of a monovalent lipid we performed additional simulations that complemented the results presented in Results and Discussion. According to Eq. 9, velocity of the peptide is proportional to its effective charge *Z*. As follows from the above discussion, *Z*, however, is a complex function of the local density of anionic lipids and cannot be easily controlled in the simulations. To lift this restriction, we varied the charge of the peptide residues beyond the physiologically relevant value of +1, in the range between +0.5 and +2.5. While the resulting positively-charged object no longer represented Lys5, as shown in Fig. S2A, velocity observed in the automaton simulations matched well the prediction of Eq. 9. To enable this comparison, the effective charge *Z* was computed at each value of the residue charge directly from the automaton simulations and then substituted into Eq. 9. Together with the results presented in Fig. 5, this demonstrates that the peptide drift observed in our automaton is fully consistent with the independently derived analytic ansatz of Eqs. 8 and 9.

Finally, we sought to validate our results using a distinct simulation strategy that does not involve our 2D two-lattice automaton. To achieve this, we constructed a coarse-grained 1D kinetic Monte-Carlo algorithm which simulated diffusion of point-wise anionic lipids and a positive charge representing the peptide on a one-dimensional lattice. Lipids interacted with the peptide via the Debye-Hueckel potential truncated at three Debye lengths, whereas the mutual interaction of lipids was neglected. Spatial coarse-graining was achieved by allowing multiple lipids to occupy the same node. To scale the results of simulations, it was assumed that an occupancy of 10 monovalent lipids per node corresponded to their molar fraction of 20%. Given this assumption the length unit corresponded to ~6 *nm*. To achieve equivalence with the standard Brownian dynamics method (without including hydrodynamics, see Sanz and Marenduzzo, 2010, J. Chem. Phys. 132:194102, and references therein), only single particle moves were used. A steady state lipid gradient was created by insertion of lipids on one boundary and their destruction upon reaching the other. Figure S2B shows that the peptide drifts up the generated lipid gradient with the velocity that is quantitatively similar to that observed in the complete 2D automaton (cf. Fig. 5C). This demonstrates that the reported effect is not an artifact of particular automaton rules (e.g., definition of the peptide and lipid moves) and is robust to the implementation details.

Effective friction reduces peptide drift velocity

The discrepancy between the apparent velocity of the peptide found in our automaton simulations and the theoretical value predicted by Eq. 9 is very intriguing. In the derivation of Eqs. 9, 10 we considered motion of the charges immediately associated with the peptide. These include intrinsic charge of the peptide amino acid residues, that of lipids bound to the

peptide and moving together with it, and, finally, charge of the lipids displaced by such a motion. Taking into the consideration our results on lipid demixing (cf. Fig. 3), motion of the peptide induces motion of a set of lipids that form the peptide-associated shell consisting of the lipids further separated from the peptide nodes and whose interaction with the peptide is significantly weaker than that of the lipids positioned directly under the peptide nodes. The drag associated with the motion of this lipid shell that continuously follows the protein moving along a large-scale lipid gradient, could potentially explain why the observed drift velocity is appreciably lower than that predicted by Eq. 9.

Construction of the qualitatively accurate theory of this phenomenon is far beyond the scope of the present study. Instead, we provide the following qualitative argument that supports the plausibility of the above hypothesis. Electrostatic potential generated by the lipids that constitute the peptide-associated shell forms a self-organized potential well that effectively stabilizes the position of the peptide in its center. An attempt of the peptide to move produces the returning force that opposes the peptide's motion and, reciprocally, pulls the potential well behind it. To further explore this idea, we consider a grossly simplified one-dimensional model system that consists of a particle diffusing under the action of an external force that simulates the effect of the lipid gradient on the membrane. This particle with diffusion coefficient D_1 is attached to another particle with which it interacts via an attractive potential V (e.g., the screened Coulomb potential through which the protein interacts with the lipids or a simple Hookean spring, see Fig. S3A for a schematic diagram). The Langevin equations of motion governing the dynamics of the system are:

$$\frac{dx}{dt} = \frac{f}{\gamma_1} - \frac{K}{\gamma_1}(x-y) + \sqrt{2D_1}\eta_1, \qquad (11)$$

$$\frac{dy}{dt} = \frac{K}{\gamma_2}(x-y) + \sqrt{2D_2}\eta_2,$$

where γ_1 and γ_2 are the friction coefficients of the first and second particles respectively, D_1 and D_2 are their diffusion coefficients, and the interaction between the two particles, for simplicity, has been modeled as a Hookean spring with constant K. Finally, $\eta_{1,2}$ are two Gaussian (white) noise terms, with variance equal to 1. Further, we introduce new variables $\zeta = x + y$ (so that the center of mass position is given by $\zeta/2$) and $\xi = x - y$. If we neglect the noise terms, and only focus on the behavior at large times, we can approximate ξ with its steady state value, which is easily found to be

$$\xi = \frac{f/\gamma_1}{K/\gamma_1 + K/\gamma_2}. \qquad (12)$$

As a consequence, the center of mass velocity v can be written as

$$v = \frac{f}{k_B T}\frac{D_1 D_2}{D_1 + D_2}, \qquad (13)$$

where we have also made use of the Stokes-Einstein's relation,

$$D_{1,2} = \frac{k_B T}{\gamma_{1,2}}.$$

Therefore the centre of mass velocity v does *not* depend on the spring constant K. Indeed, it can be shown that v does not depend at all on the shape of the potential. Illustrating this fact, Fig. S3B shows kinetic Monte-Carlo simulations of the system of two particles interacting via the sum of a spring and a finite-radius electrostatic potential V' of variable size defined as follows:

$$V' = \begin{cases} \varepsilon r_0 \left[\dfrac{e^{-\frac{r}{\lambda}}}{r + r_0} - \dfrac{e^{-\frac{r_C}{\lambda}}}{r + r_0} \right], \; r < r_C \\ 0, \; r > r_C \end{cases}, \tag{14}$$

where $r_C = 3\lambda$. The most relevant prediction of our simplified model for the lateral dynamics of the peptide on the membrane is that a particle interacting with a lipid shell should move slower due to the combined drag term that is presented above and equals to $k_B T (D_1 + D_2)/D_1 D_2$. Therefore, any finite effective diffusivity for the lipid shell arising from lipid demixing will diminish effective mobility of the peptide, for instance, in a lipid concentration gradient. We believe that this effect could qualitatively explain the effective coefficient ϑ that was found in fitting the simulation results to the theory. Finally, it should be noted that a similar analysis can be performed also in the absence of a pulling force with the same result demonstrating that a system of two attractively interacting particles diffuses with the effective diffusion coefficient $D = D_1 D_2 / (D_1 + D_2)$.

Supporting Figures

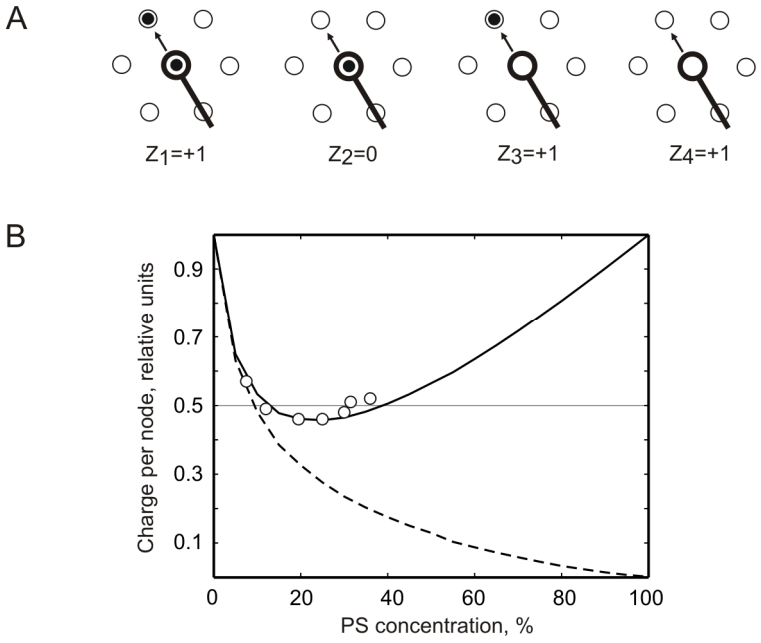

Figure S1. The value of the effective charge Z in Eq. 8 that translocates during the drift of the peptide is a weak function of the local PS concentration. (A) The four possible elementary translational moves of a peptide node (shown by thick line) projected onto the lipid lattice. Solid circle within the lipid lattice node represents a PS lipid. (B) The value predicted by Eq. 10 (solid line) is compared to the simulation results (open circles). The total charge of the peptide together with the associated lipids is shown by the dashed line.

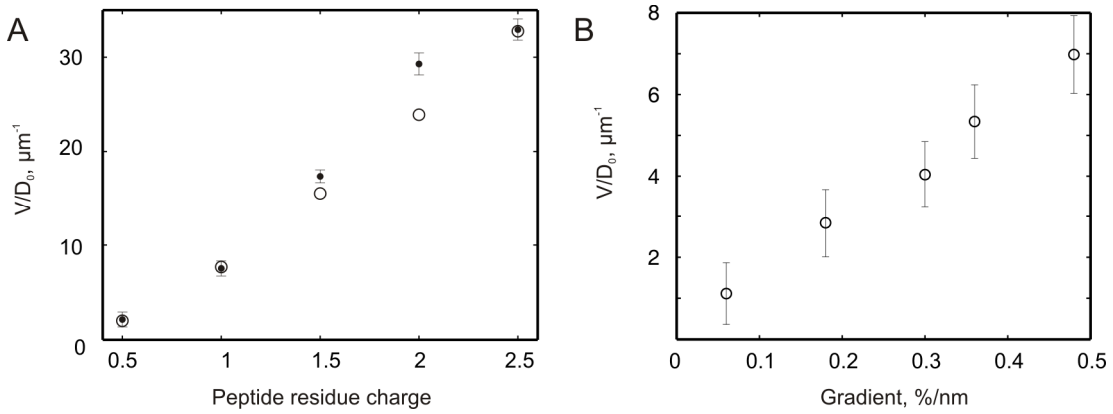

Figure S2. Peptide drift in the gradient of a monovalent lipid. (A) Dependence of the peptide velocity on the peptide residue charge. The peptide diffusion coefficient and the lipid gradient are $0.2D_0$ and $0.6\%/nm$, respectively. Simulation results (filled circles) are compared to the values predicted by Eq. 9 (open circles). (B) Velocity of the peptide drift is proportional to the lipid gradient also in the coarse-grained 1D Monte-Carlo model (see text for details).

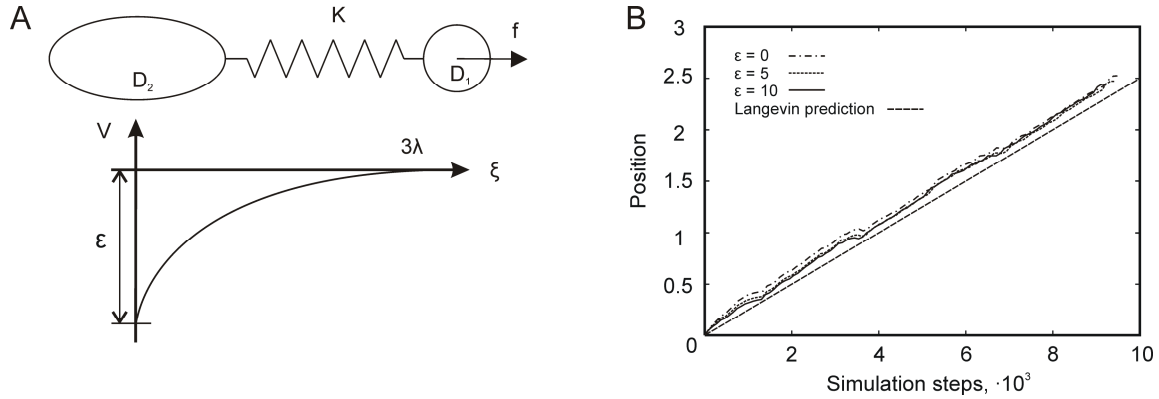

Figure S3. Drift of a particle together with the associated potential well. (A) A sketch of the hypothetical system that consists of a particle (the peptide) that diffuses under the action of a force *f* while associated with a second particle (lipid shell) via the interaction potential *V* symbolically depicted as a spring with constant *K*. (B) Results of 1D Monte-Carlo simulations for the system shown in A where *V* is given by Eq. 14. All quantities are in arbitrary nondimensional units. Time has been rescaled by the Monte-Carlo acceptance rate as suggested in (Sanz and Marenduzzo. 2010. J. Chem. Phys. 132:194102).